Journal of Power Sources 183 (2008) 62–68

Contents lists available at ScienceDirect

Journal of Power Sources

journal homepage: www.elsevier.com/locate/jpowsour

Effect of preparative parameters on the characteristic of poly(vinylidene fluoride)-based microporous layer for proton exchange membrane fuel cells

Ai Lien Ong, Aldo Bottino*, Gustavo Capannelli, Antonio Comite

Dipartimento di Chimica e Chimica Industriale, via Dodecaneso 31, 16146 Genova, Italy

ARTICLE INFO

Article history:
Received 19 February 2008
Received in revised form 14 April 2008
Accepted 27 April 2008
Available online 4 May 2008

Keywords:
PVDF
Microporous layer
Gas diffusion layer
Electrically conductive filler
PEM fuel cell

ABSTRACT

The effect of preparative parameters on the characteristic of PVDF-based microporous layers (MPL) for proton exchange membrane (PEM) fuel cell was investigated. Physical properties of MPL involving electrical resistance, gas permeability and microstructure were examined. The results show that the characteristics of MPL were affected by preparative parameters, such as PVDF concentration, type of electrically conductive filler and its loading, PVDF/electrically conductive filler ratio, as well as type of PVDF solvent. The PEM fuel cell performance test demonstrates that the obtained MPL has a great potential and interest for further study and development.

1. Introduction

In responding to the challenge of satisfying the rapid increase in the global demand of energy while developing environment friendly forms of power generation to reduce air pollution and lessen the threat of global warming, proton exchange membrane fuel cells (PEMFC) are becoming one of the potential alternative power sources. However, the prohibitive cost of the PEMFC in conjunction with the problem of low reliability and durability presently are the major obstacles to its commercialization [1–3]. The performance and cost of a PEMFC are critically dependent on the electrocataytic activity of the noble metal platinum (Pt) catalyst [4–6], as well as on material selection, fabrication processes and performance of its various components, such as proton exchange membrane (PEM) [7–9], gas diffusion layers (GDL) [10–12] and bipolar plates [13–15].

PEM also called as catalyst-coated membrane if the electrocatalyst is formerly attached to the PEM, requires a certain amount of water for high proton conduction; however, the exceeding water can be easily condensed to liquid water phase within the gas diffusion electrodes, in which this phenomena is defined as water flooding [16,17]. This liquid water phase may drastically decrease the PEMFC performance by hindering gas diffusion, as well as by covering the active sites of the electrocatalysts, forming a dead reaction zone [16–19]. Therefore, the porous GDL is one of the key components in PEMFC, as it promotes effective transportation of gas reactants to the catalyst layers, providing low electronic resistance (due to its surface that enhances good electronic contact between bipolar plate and catalyst), allowing an optimal catalyst utilization. Finally, it ensures an efficient water management allowing water-flooding prevention because of its proper hydrophobicity. A GDL consists of a gas diffusion-backing layer, also called macroporous substrate, made of either a woven carbon cloth or a non-woven carbon paper (due to their good electrical conductivity, porosity and mechanical strength) with or without microporous layer (MPL).

The MPL is an electrically conductive layer, commonly composed by carbon black powder and hydrophobic agent. It can be applied on one side or both sides of the gas diffusion-backing layer. The role of MPL is to enhance further the performance of a GDL by minimizing electronic contact resistance, improving gas transport and reducing the water-flooding tendency thanks to a proper structure, pore size and distribution and also its hydrophobic character. The improved performance of a GDL, due to the presence of MPL, is a recent subject of extensive attention. Aityeh et al. [20] reported that PEMFC with a carbon–polytetrafluoroethylene (PTFE) MPL on either electrode or on both electrodes provided a better overall performance and durability compared to cells without a MPL. Zhan et al. [21] analyzed the distribution of liquid water phase saturation for different GDL structures and concluded that gas diffusion increased with the increase of porosity as well as the porosity gradient along the MPL thickness. Tang et al. [22]

* Corresponding author. Tel.: +39 0103538724; fax: +39 0103538759.
E-mail address: bottino@chimica.unige.it (A. Bottino).

0378-7753/$ – see front matter © 2008 Published by Elsevier B.V.
doi:10.1016/j.jpowsour.2008.04.064

found that the PEMFC consisting of through-plane porosity-graded carbon–PTFE MPL have better performance than those consisting of conventional homogeneous MPL, especially at high current densities. Kong et al. [19] demonstrated that pore size distribution of MPL was the crucial parameter for mass transport processes within gas diffusion electrodes, as well as for cell performance characteristic than the overall porosity. Gurau et al. [23] found that the in-plane and through-plane viscous permeability coefficient of commercial macroporous substrates and carbon–PTFE MPL-coated GDLs depended on the type of carbon and increased with increasing the PTFE content in the GDL. Chen et al. [17] suggested that the carbon–PTFE with in-plane MPL coating gradients established a more uniform water distribution and could effectively avoid any drying-out of polyelectrolyte at the cell inlet, as well as the cathode flooding at the cell outlet. Many studies have been carried out on the effect of electrically conductive filler on MPL microstructure and performance, in terms of carbon loading [24,25], carbon loading configuration [26], carbon type [27], composite carbon black [28,29] and adoption of nano-materials [16]. As a consequence, different interpretations and optimal experimental results were obtained independently.

As shown above, a lower effort has been paid to discover an alternative hydrophobic binding agent for MPL. The majority of gas diffusion electrodes use PTFE as a hydrophobic binder, due to its superior thermal stability and resistance to chemical degradation. However, PTFE preparations mostly require high sintering temperature process from powder or suspension, because of its insolubility in any known solvent; this contributes to the cost of PEMFC. With the aim of producing a low-cost, easy to prepare gas diffusion electrodes with favorable chemical and electrical properties, a method for obtaining gas diffusion electrodes based on poly(vinylidene fluoride) (PVDF)–carbon blends via phase inversion was firstly detailed by Cabasso et al. [30]. A further improvement was reached by Hitomi [31], who obtained an improved percent utilization of catalyst in gas diffusion electrodes studies. Unfortunately, only a handful studies on this type of hydrophobic binding agents have been carried out since then. This motivates the present studies, particularly for MPL. Our objective is a deeper and better understanding of the effect of preparative parameters on the characteristic of PVDF-based MPL for PEMFC. Physical properties of PVDF-based MPL, including resistance, through-plane gas permeability and the resulted microstructure were carefully examined. For a better overview, a performance analysis of the PVDF-based MPL-coated GDL was carried out as well.

2. Experimental

2.1. Preparation of PVDF-based MPL

The MPLs were prepared by phase inversion technique [32] using PVDF as hydrophobic binding agent with carbon black (Vulcan XC-72R, Cabot Inc.) and/or graphite (Timrex HSAG 300, TIMCAL) as electrically conductive filler. The electrically conductive filler was dispersed in a PVDF solution obtained by dissolving the polymer in *N*,*N*-dimethylformamide (DMF) or *N*-methyl-2-pyrrolidone (NMP). The casting dispersion was mixed alternately using an ultrasonic bath and a magnetic stirrer for at least 3 days, forming slurry that was successively cast at room temperature, as a thin film, with a knife onto a smooth glass-plate or a commercially available wet-proof carbon cloth gas diffusion-backing layer (E-TEK Division) under an appropriately controlled slurry thickness. Extra care was taken during the casting to make sure the slurry only partially penetrated the gas diffusion-backing layer. After a 30 s exposure period, the film was immersed into a water bath to form the MPL that was leached extensively with deionized water before drying at room temperature. MPL with different thickness were obtained by varying the thickness of the cast slurry film.

2.2. Preparation of traditional PTFE MPL on carbon cloth substrate

To prepare carbon ink for MPL, carbon powder (0.4 g, Vulcan XC-72R) was mixed with 40% PTFE-dispersed water, isopropyl alcohol (25 mL) and glycerol (0.8 mL) in an ultrasonic bath for 2 h. The resulting carbon ink was brush-deposited onto one side of wet-proof carbon cloth gas diffusion-backing layer (E-TEK Division), and successively dried at 80 °C for 30 min. The GDL sample was heat-treated at 280 °C for 30 min to evaporate all remaining glycerol, then at 350 °C for 30 min to distribute homogeneously PTFE throughout the MPL. In the MPL, the carbon loading was about 6 mg cm^{-2}.

2.3. Resistance measurement

The through-plane resistance of MPL was measured at 25 °C by using a 2-point resistance measurement device, Keithley 2000 Multimeter (Keithley Instruments Inc.), fitted with two copper cylindrical plates blocking the sample (surface area of 0.20 cm^2). Prior to resistance measurements, the two copper cylindrical plates were pretreated with metal polish wadding followed by acetone cleaning to remove any surfaces' contaminants. A current was passed through the cell and the voltage drop across the MPL sample was measured. The measured resistance values represent the overall resistance of the sample and the two contact resistances between samples and the copper plates.

2.4. Through-plane air permeability measurement

The through-plane air permeability was determined at 25 °C temperature by measuring the pressure drop through MPL corresponding to a given air flux preset by a mass flow device. The MPL surface area was 0.80 cm^2.

2.5. Scanning electron microscopy

A LEO Stereoscan 440 (LEO Electron Microscopy Ltd.) scanning electron microscope (SEM) equipped with analytical system of EDS (Oxford link with a Ge detector with the resolution of 120 eV) was used at accelerating voltages of 1 and 30 kV. Dried MPL samples were fractured at liquid nitrogen temperature and fixed to a SEM spin stub with a conductive adhesive prior to be coated with a thin layer of gold (20 nm) by using a sputtering device. MPL images were taken at different magnifications.

2.6. Membrane–electrode assemblies and PEM fuel cell test

Commercially available catalyst-coated membrane (PAXITECH Co.) consisting of a Nafion® 212 membrane (DuPont) with a Pt loading of 0.5 mg cm^{-2} for both anode and cathode side was used to investigate the single cell performance of the MPL samples. The membrane–electrode assembly was constructed with the PVDF-based MPL-coated GDL only at the cathode and a wet-proof commercially available gas diffusion-backing layer at the anode. In order to make a comparison, the wet-proof commercial gas diffusion-backing layer and traditional PTFE MPL-coated GDL were used at the cathode instead of PVDF-based MPL-coated GDL.

The performance of the single cell with the active area of 5 cm^2 was measured with H_2 as fuel gas and air as oxidant at 60 °C without back pressure in a fuel cell test station (Fideris Innovative Solutions) equipped with SCADA (Supervisory Control and Data Acquisition) system. The external humidification temperatures of H_2 and air were constantly kept at 70 and 65 °C, respectively. H_2

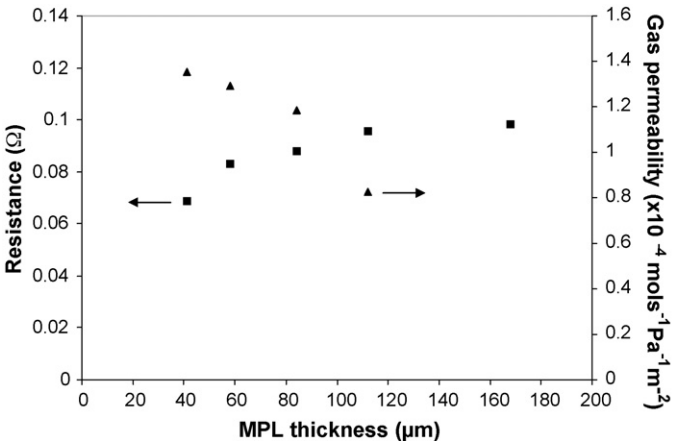

Fig. 1. Effect of MPL thickness on resistance and gas permeability.

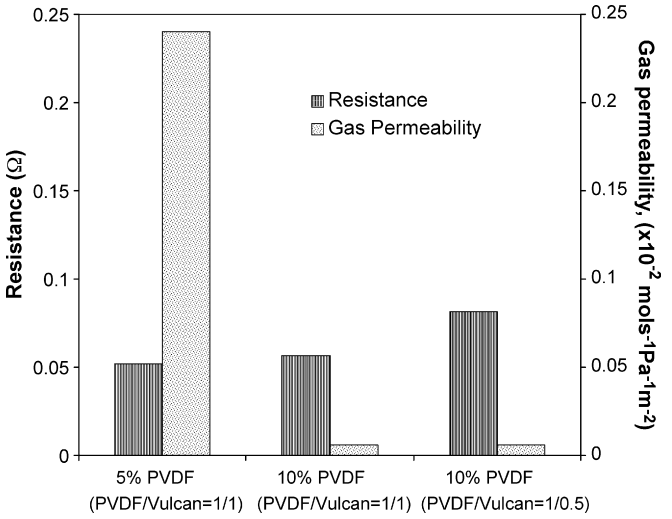

Fig. 3. Effect of PVDF concentration in DMF and PVDF/electrically conductive filler ratio on MPL resistance and gas permeability.

and air flow rates of 0.2 L min^{-1} were fed. Prior to the polarization curves recording, assembled cells were activated by setting polarization at ramp mode and operate continuously till a stable performance was obtained.

3. Results and discussion

3.1. Effect of MPL thickness

MPL thickness was measured by micrometer with an accuracy of 1 μm. In order to obtain reliable results, thickness measurements have been performed using three different samples from the same batch of MPL and the mean-value was calculated. The same approach was followed for resistance and gas permeability measurements as well. Fig. 1 shows the effect of MPL thickness on resistance and gas permeability. As expected, resistance increases (from 0.069 to 0.096 Ω) with the increase of MPL thickness (from 41 to 112 μm) and almost levels off at 0.096 Ω with further increase in the MPL thickness. In contrast with resistance, MPL gas permeability decreases from 1.35 to 0.83×10^{-4} mol s^{-1} Pa^{-1} m^{-2} with the increase of MPL thickness from 41 to 112 μm within the studied range.

The behavior of resistance and gas permeability can be explained as a function of MPL thickness through the inspection of SEM images reported in Fig. 2. The MPL with lower thickness (Fig. 2a$_1$ and b$_1$) possess almost homogenous through-plane porosity with cavities throughout the cross-section and higher amount

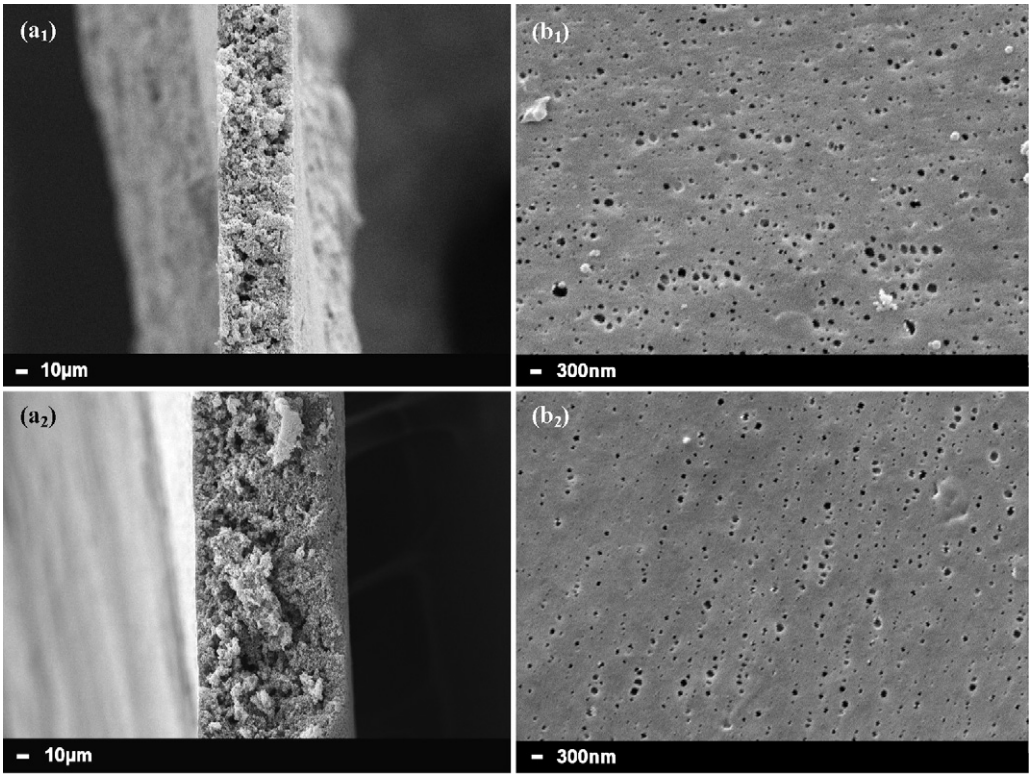

Fig. 2. SEM images of cross-section (a) and surface (b) of MPLs with different thickness.

of larger pores on the surface (corresponding to the air–slurry interface). Thus, the MPL matrix has resulted to lower material resistance, while the higher porosity and lower thickness yield better gas permeability. On the contrary, the thicker MPL (Fig. 2a_2 and b_2) presents inhomogeneous through-plane porosity with visualable compact layer (on the right side of the SEM image) and smaller pore size on its surface that increases the MPL resistance and reduces gas permeability.

The observed results can be attributed to the different membrane mechanism formation during water immersion step. Phase separation during water immersion is a very complicated polymer precipitation process, controlled by the polymer solvent–water exchange as well as by shrinkage phenomena. Binary solutions, composed of polymer and solvent, are free to shrink during water immersion; consequently very small pores are formed on the membrane surface [32]. The addition of particles to binary polymer solutions alters the phase separation process, as particles do not obviously shrink during membrane formation in the water bath. As a result, new large pores are formed on the membrane surface [33,34] and their number and size increases with the increase of the particles concentration in the dispersion [34]. However, during the exposure period of the cast dispersion before water immersion, particle settling phenomena can occur (especially when the dispersion viscosity is low), thus leading to polymer enrichment at the air-cast dispersion. By increasing the thickness of the cast dispersion, a thicker polymer rich layer is formed; consequently the surface of the resulting membrane becomes less porous.

3.2. Effects of PVDF concentration and PVDF/electrically conductive filler ratio

Fig. 3 is a plot of MPL resistance and gas permeability as a function of PVDF concentration and PVDF/electrically conductive filler ratio. In the case of the MPL with PVDF/electrically conductive filler ratio of 1/0.5, resistance increases from 0.052 to 0.082 Ω with the increase of PVDF concentration from 5% to 10%; the gas permeability drops significantly from 23.99 to 0.57×10^{-4} mol s^{-1} Pa^{-1} m^{-2}. Nevertheless, at a constant PVDF concentration (10%), MPL resistance decreases with the decrease of PVDF/electrically conductive

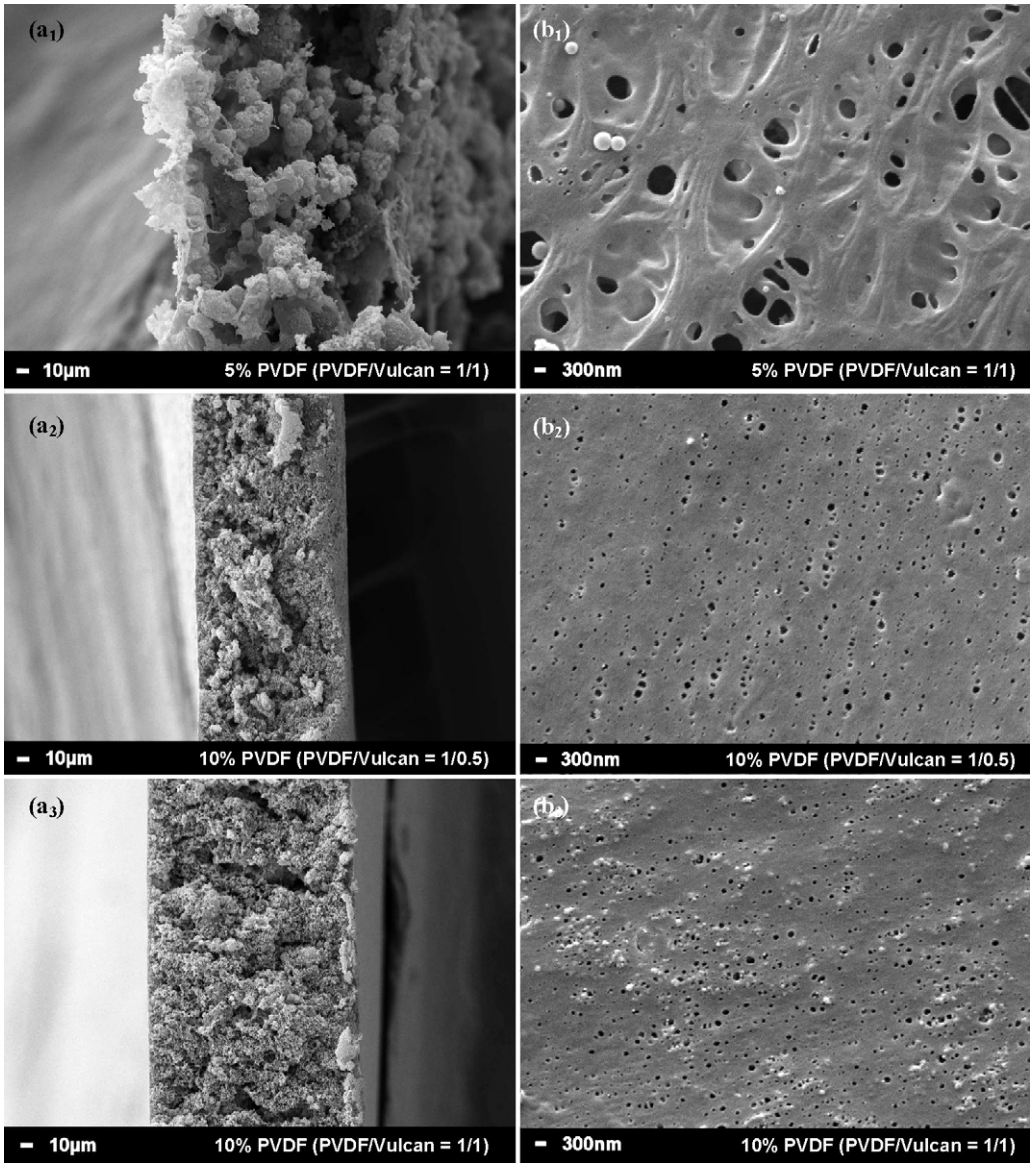

Fig. 4. SEM images of cross-section (a) and surface (b) of MPLs prepared by different PVDF concentration in DMF and PVDF/electrically conductive filler ratio.

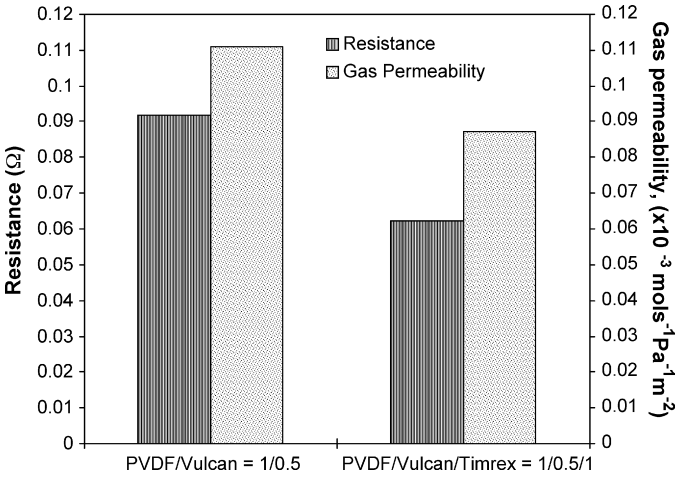

Fig. 5. Effect of electrically conductive filler blend on MPL resistance and gas permeability.

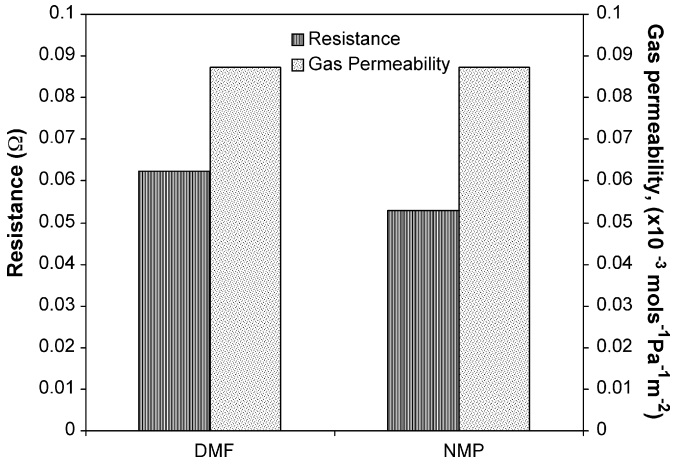

Fig. 7. Effect of PVDF solvent on MPL resistance and gas permeability.

filler ratio, whereas the influence on gas permeability is not relevant.

The inspection of SEM images shown in Fig. 4 reveals clearly that the PVDF concentration and PVDF/electrically conductive filler ratio have a considerable effect on MPL structure, which explains the variation in MPL resistance and gas permeability. A very low PVDF leads to a MPL with a very inhomogeneous cross-section structure (Fig. 4a_1) and very large surface pore (Fig. 4b_1), that yields very high gas permeability. At a higher PVDF concentration (Fig. 4a_2), the MPL structure is significantly packed down with very small surface pore (Fig. 4b_2), resulting in lower gas permeability. It is worth remembering that PVDF is not a conductive polymer. Thus, an increase of polymer concentration has a positive effect on hydrophobicity as well as on mechanical properties and unfortunately, also on the material resistance. On the contrary, by keeping the PVDF concentration constant and by decreasing the PVDF/electrically conductive filler ratio, the MPL porosity increases due to the formation of cavities along its cross-section (Fig. 4a_3) and of a larger amount of bigger pores on the surface (Fig. 4b_3). In addition, an increase of thickness is observed. Therefore, higher electrically conductive filler content reduces the MPL resistance, with a mild impact on gas permeability.

3.3. *Effect of electrically conductive filler blend*

Since the addition of large amount of Vulcan led to slurry that was quite impossible to cast (owing to its high viscosity), it was decided to prepare high electrically conductive filler loading slurry by using a blend of carbon black (Vulcan) and graphite (Timrex)

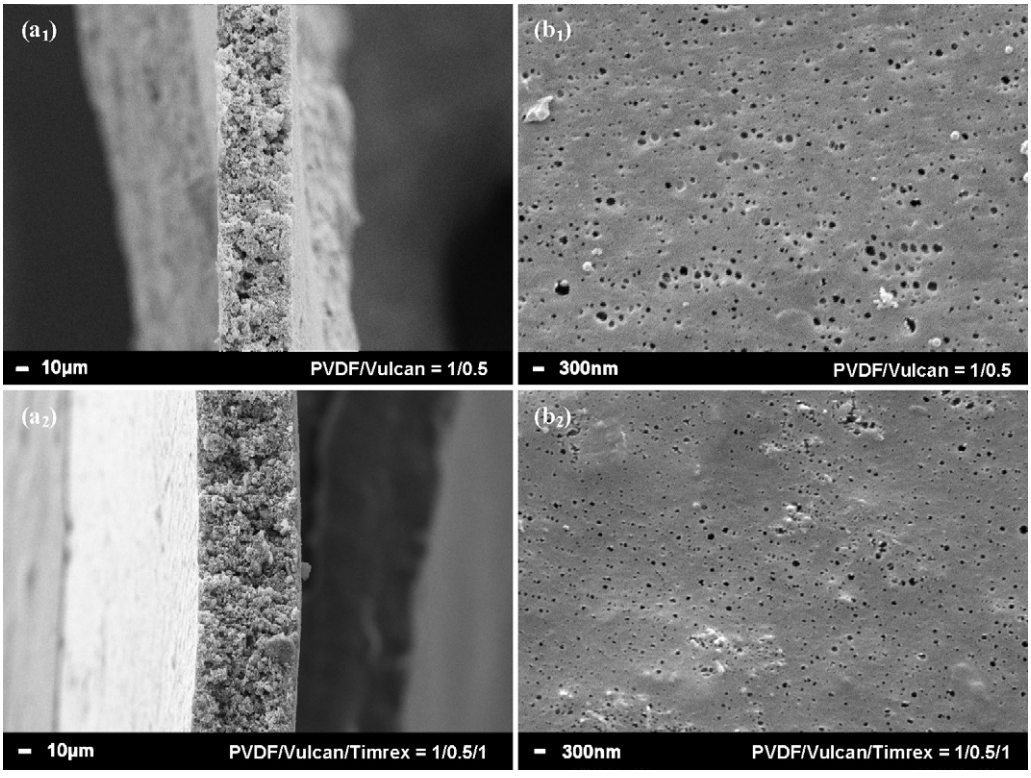

Fig. 6. SEM images of cross-section (a) and surface (b) of MPLs prepared from different electrically conductive filler.

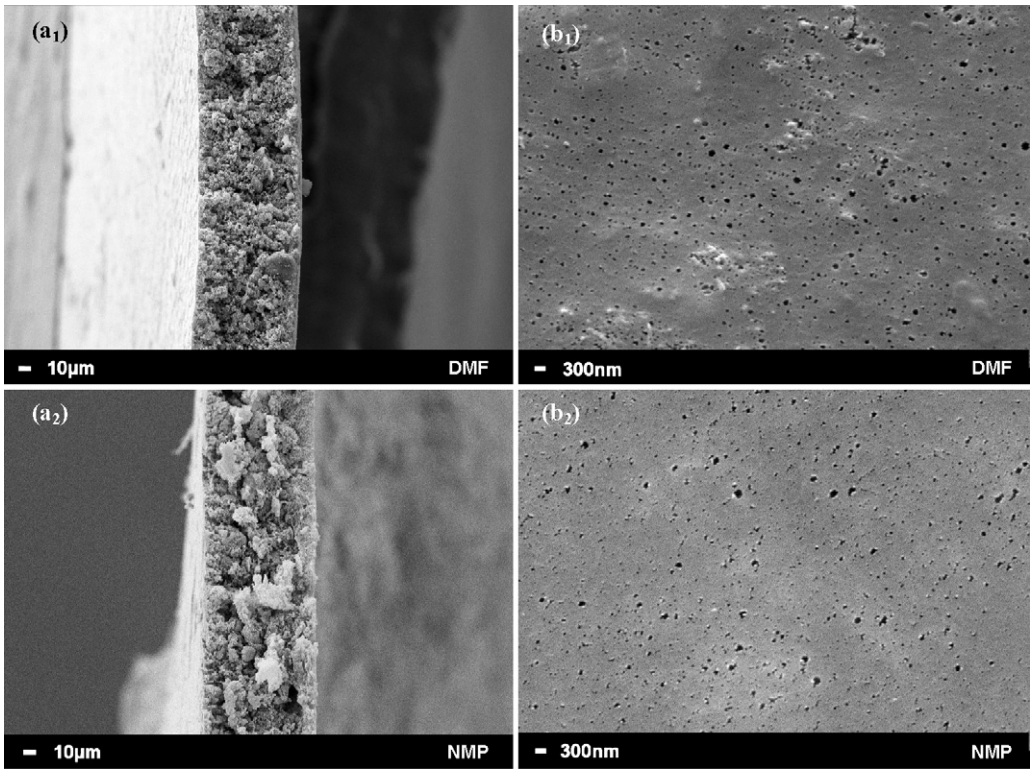

Fig. 8. SEM images of cross-section (a) and surface (b) of MPLs prepared by different PVDF solvent.

particles, the size of which is much larger than that of Vulcan particles. A lower contribution to the viscosity increase is consequently predicted. The effect of electrically conductive filler blend on resistance and gas permeability of MPL is shown in Fig. 5. As it can be seen, the use of electrically conductive filler blend reduces resistance from 0.092 to 0.062 Ω, though it also causes gas permeability of MPL to drop gently from 1.11 to 0.87 $\times 10^{-4}$ mol s^{-1} Pa^{-1} m^{-2}.

Fig. 6 shows the effect of electrically conductive filler blend on the structure of MPL. Addition of Timrex in the blend does not seem to alter significantly the structure and porosity of MPL, but it leads to a slight increase of MPL thickness. So, the positive effect on electrical conductivity due to the addition of Timrex is associated to a slightly negative influence on air permeability.

3.4. Effect of PVDF solvent

Fig. 7 compares the properties of MPL prepared by using different PVDF solvent (DMF and NMP). As it can be seen, the type of solvent has a significant impact on MPL resistance and gas permeability. DMF cast MPL posses higher resistance (0.062 Ω) than the NMP cast MPL (0.053 Ω). Nevertheless, both DMF and NMP cast MPLs present very close gas permeability values.

These results can be reasonably explained with the SEM micrographs reported in Fig. 8. In fact, the MPL cast from DMF slurry shows a more compact cross-section structure, but the size and the number of the surface pores does not differ too much from the NMP cast MPL.

3.5. PEM fuel cell performance evaluation

Fig. 9 compares the polarization curves of blank commercial GDL, traditional PTFE MPL-coated GDL and PVDF-based MPL-coated GDL. The performance of commercial GDL coated with PVDF-based MPL is better than that of blank commercial GDL and commercial GDL coated with traditional PTFE MPL, especially at high current densities (>ca. 0.3 A cm^{-2}). Gas mixture is transported by convection from the cathode flow-field, through the GDL towards the catalyst layer while the produced liquid water must be transported in counter-flow from the catalyst layer, through the GDL into the cathode flow-field [23]. According to Litster et al. [35], the liquid water transport within GDL is a process of pressure buildup and breakthrough. Capillary forces are the main resistance to the liquid–gas interface progression in the hydrophobic structure. Therefore, the fluid will preferentially pass through the cross-sections featuring the greatest spacing, as this reduces capillary pressure resistance [35]. In addition, the gas mixture distribution in the flow-field can be super-positioned by a flow in the GDL [36]. Thus, better mass transport at higher current densities region was achieved for GDL at the presence of PVDF-based MPL (Fig. 9), due to its appropriate in-plane and through-plane

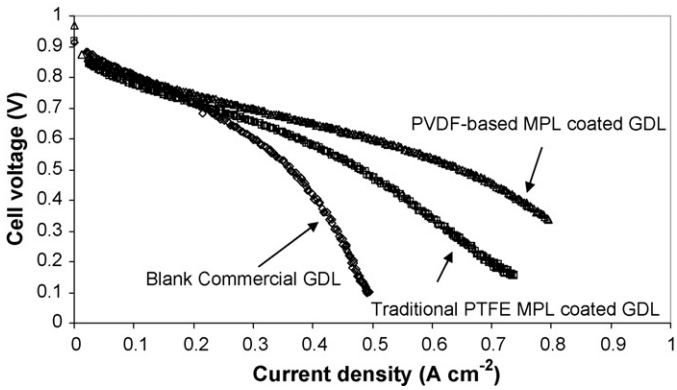

Fig. 9. Polarization curves of blank commercial GDL, traditional PTFE MPL-coated GDL and PVDF-based MPL-coated GDL.

microstructures. The PVDF-based MPL has a hydrophobic asymmetric porous structure with cavities, in which the in-plane and through-plane mass transport enhanced. This effect is obviously not present in the conventional PTFE MPL and without MPL-coated GDLs. Hence, the obtained results demonstrate that the PVDF-based MPL has a great potential and interest for further study and development.

4. Conclusion

A large variety of MPL has been prepared from slurries formed by an intimate dispersion of electrically conductive filler into a PVDF solution. The effect of preparative parameters such as PVDF concentration, PVDF/electrically conductive filler ratio and PVDF solvent on MPL thickness, resistance and gas permeability has been investigated. The PEMFC performance test demonstrates that the presence of PVDF-based MPL potentially reduces mass transport losses within the GDL at current densities higher than ca. 0.3 A cm^{-2}. Thus, these findings justify future studies and continuous improvement of PVDF-based MPL.

References

[1] C.W.B. Bezerra, L. Zhang, H. Liu, K. Lee, A.L.B. Marques, W.P. Marques, H. Wang, J. Zhang, J. Power Sources 173 (2007) 891–908.
[2] Y. Zhang, R. Pitchumani, Int. J. Heat Mass Transf. 50 (2007) 4698–4712.
[3] Y. Shao, G. Yin, Y. Gao, J. Power Sources 171 (2007) 558–566.
[4] X. Yu, S. Ye, J. Power Sources 172 (2007) 145–154.
[5] B. Moreno, E. Chinarro, J.C. Pérez, J.R. Jurado, Appl. Catal. B: Environ. 76 (2007) 368–374.
[6] H. Park, Y. Cho, Y. Cho, C.R. Jung, J.H. Jang, Y. Sung, Electrochim. Acta 53 (2007) 763–767.
[7] H. Tang, X. Wang, M. Pan, F. Wang, J. Membr. Sci. 306 (2007) 298–306.
[8] S.B. Brijmohan, M.T. Shaw, J. Membr. Sci. 303 (2007) 64–71.
[9] Y. Sato, K. Fujii, N. Mitani, A. Matsuura, T. Kakigi, F. Muto, J. Li, A. Oshima, M. Washio, Nucl. Instrum. Methods B 265 (2007) 213–216.
[10] Y.W. Chen-Yang, T.F. Hung, J. Huang, F.L. Yang, J. Power Sources 173 (2007) 183–188.
[11] P.K. Sinha, C. Wang, Electrochim. Acta 52 (2007) 7936–7945.
[12] Y. Zhou, G. Lin, A.J. Shih, S.J. Hu, J. Power Sources 163 (2007) 777–783.
[13] K.M. Kim, K.Y. Kim, J. Power Sources 173 (2007) 917–924.
[14] K.S. Weil, G. Xia, Z.G. Yang, J.Y. Kim, Int. J. Hydrogen Energy 32 (2007) 3724–3733.
[15] T. Fukutsuka, T. Yamaguchi, S. Miyano, Y. Matsuo, Y. Sugie, Z. Ogumi, J. Power Sources 174 (2007) 199–205.
[16] G. Park, Y. Sohn, S. Yim, T. Yang, Y. Yoon, W. Lee, K. Eguchi, C. Kim, J. Power Sources 163 (2006) 113–118.
[17] J. Chen, T. Matsuura, M. Hori, J. Power Sources 131 (2004) 155–161.
[18] J. Benzigerr, J. Nehlsen, D. Blackwell, T. Brennan, J. Itescu, J. Membr. Sci. 261 (2005) 98–106.
[19] C.S. Kong, D. Kim, H. Lee, Y. Shul, T. Lee, J. Power Sources 108 (2002) 185–191.
[20] H.K. Atiyeh, K. Karan, B. Peppley, A. Phoenix, E. Halliop, J. Pharoah, J. Power Sources 170 (2007) 111–121.
[21] Z. Zhan, J. Xiao, Y. Zhang, M. Pan, R. Yuan, Int. J. Hydrogen Energy 32 (2007) 4443–4451.
[22] H. Tang, S. Wang, M. Pan, R. Yuan, J. Power Sources 166 (2007) 41–46.
[23] V. Gurau, M.J. Bluemle, E.S.D. Castro, Y. Tsou, T.A. Zawodzinski, J.A. Mann, J. Power Sources 165 (2007) 793–802.
[24] S. Park, J. Lee, B.N. Popov, J. Power Sources 163 (2006) 357–363.
[25] M. Han, S.H. Chan, S.P. Jiang, J. Power Sources 159 (2006) 1005–1014.
[26] E. Antolini, R.R. Passos, E.A. Ticianelli, J. Power Sources 109 (2002) 477–482.
[27] L.R. Jordan, A.K. Shukla, T. Behrsing, N.R. Avery, B.C. Muddle, M. Forsyth, J. Power Sources 86 (2000) 250–254.
[28] X. Wang, H. Zhang, J. Zhang, H. Xu, X. Zhu, J. Chen, B. Yi, J. Power Sources 162 (2006) 474–479.
[29] X.L. Wang, H.M. Zhang, J.L. Zhang, H.F. Xu, Z.Q. Tian, J. Chen, H.X. Zhong, Y.M. Liang, B.L. Yi, Electrochim. Acta 51 (2006) 4909–4915.
[30] I. Cabasso, Y. Yuan, X. Xu, US 5,783,325 (1998).
[31] S. Hitomi, US 2001/0,041,283 A1 (2001).
[32] A. Bottino, G. Camera-Roda, G. Capannelli, S. Munari, J. Membr. Sci. 57 (1991) 1–20.
[33] A. Bottino, G. Capannelli, A. Comite, Desalination 146 (2002) 35–40.
[34] P. Aerts, I. Genne, S. Kuypers, R. Leysen, I.F.J. Vankelecom, P.A. Jacobs, J. Membr. Sci. 178 (2000) 1–11.
[35] S. Litster, D. Sinton, N. Djilali, J. Power Sources 154 (2006) 95–105.
[36] H. Dohle, R. Jung, N. Kimiaie, J. Mergel, M. Muller, J. Power Sources 124 (2003) 371–384.